PCCP

PAPER

View Article Online
View Journal | View Issue

Cite this: *Phys. Chem. Chem. Phys.*, 2015, **17**, 25772

Gas-phase VUV photoionisation and photofragmentation of the silver deuteride nanocluster $[Ag_{10}D_8L_6]^{2+}$ (L = bis(diphenylphosphino)methane). A joint experimental and theoretical study†

Steven Daly,[a] Marjan Krstić,[b] Alexandre Giuliani,[cd] Rodolphe Antoine,[a] Laurent Nahon,[c] Athanasios Zavras,[ef] George N. Khairallah,[ef] Vlasta Bonačić-Koutecký,*[bg] Philippe Dugourd*[a] and Richard A. J. O'Hair*[ef]

Received 26th February 2015,
Accepted 20th March 2015

DOI: 10.1039/c5cp01160d

www.rsc.org/pccp

The bis(diphenylphosphino)methane (L = $Ph_2PCH_2PPh_2$) ligated silver deuteride nanocluster dication, $[Ag_{10}D_8L_6]^{2+}$, has been synthesised in the condensed phase *via* the reaction of bis(diphenylphosphino)methane, silver nitrate and sodium borodeuteride in the methanol : chloroform (1 : 1) mixed solvent system. The photoionisation and photofragmentation of this mass-selected cluster were studied using a linear ion trap coupled to the DESIRS VUV beamline of the SOLEIL Synchrotron. At 15.5 eV the main ionic products observed are $[Ag_{10}D_8L_5]^{2+}$, $[Ag_{10}D_8L_4]^{2+}$, $[Ag_{10}D_8L_6]^{3+\bullet}$, $[Ag_9D_8L_4]^{2+\bullet}$, and $[AgL_2]^+$. The later two products arise from fragmentation of $[Ag_{10}D_8L_6]^{3+\bullet}$. An analysis of the yields of these product ions as a function of the photon energy reveals the onset for the formation of $[AgL_2]^+$ and $[Ag_9D_8L_4]^{2+\bullet}$ is around 2 eV higher than that for ionisation to produce $[Ag_{10}D_8L_5]^{3+\bullet}$. The onset of ionisation energy of $[Ag_{10}D_8L_6]^{2+}$ was determined to be 9.3 ± 0.3 eV from a fit of the yield of the product ion, $[Ag_{10}D_8L_6]^{3+\bullet}$, as a function of the VUV photon energy. DFT calculations at the RI-PBE/RECP-def2-SVP level of theory were carried out to search for a possible structure of the cluster and to estimate its vertical and adiabatic ionisation energies. The calculated lowest energy structure of the $[Ag_{10}D_8L_6]^{2+}$ nanocluster contains a symmetrical bicapped square antiprism as a silver core in which hydrides are located as a mix of triangular faces and edges. Four of the bisphosphines bind to the edges of the cluster core as bidentate ligands, the remaining two bisphosphines bind *via* a single phosphorus donor atom to each of the apical silver atoms. The DFT calculated adiabatic ionisation energy for this structure is 8.54 eV, in satisfactory agreement with experiment.

Introduction

Although silver hydride nanoclusters are key intermediates in reactions involving organic substrates in both the gas[1] and condensed phases,[2] they have largely eluded structural characterization in the gas[3] and condensed phases[4] until recent reports employing spectroscopic techniques and X-ray crystallography. We have used electrospray ionisation mass spectrometry (ESI-MS) as a key discovery tool to: (i) examine the types of silver hydride nanoclusters formed upon the reaction of silver salts, bisphosphine ligands and sodium borohydride;[5] (ii) probe their gas-phase structure[3a,b] and reactivity;[5] and (iii) to direct the solution phase synthesis and characterization of these nanoclusters. ESI-MS provides evidence for the formation of the following silver nanoclusters: $[Ag_3HL_3]^{2+}$, $[Ag_3Cl_2L_3]^+$, $[Ag_3HClL_3]^+$, and $[Ag_{10}H_8L_6]^{2+}$ (L = bis(diphenylphosphino)methane, $(Ph_2P)_2CH_2$, dppm). With the exception of the last nanocluster, all of these have been isolated as salts in the condensed phase and structurally characterised *via* IR, NMR and X-ray crystallography.

[a] *Institut Lumière Matière, Université Claude Bernard Lyon 1, CNRS UMR 5306, Lyon, France. E-mail: philippe.dugourd@univ-lyon1.fr*
[b] *Center of Excellence for Science and Technology – Integration of Mediterranean region (STIM) at Interdisciplinary Center for Advanced Science and Technology (ICAST), University of Split, Meštrovićevo šetalište 45, Split, Croatia*
[c] *SOLEIL, l'Orme des Merisiers, St Aubin BP48, F-91192 Gif sur Yvette, Cedex, France*
[d] *INRA, UAR1008 Caractérisation et Élaboration des Produits Issus de l'Agriculture, F-44316 Nantes, France*
[e] *School of Chemistry and Bio21 Molecular Science and Biotechnology Institute, University of Melbourne, 30 Flemington Rd, Parkville, Victoria 3010, Australia. E-mail: rohair@unimelb.edu.au*
[f] *ARC Centre of Excellence for Free Radical Chemistry and Biotechnology, The University of Melbourne, Victoria 3010, Australia*
[g] *Humboldt-Universität Berlin, Institut für Chemie, Berlin, Germany. E-mail: vbk@cms.hu-berlin.de*

† Electronic supplementary information (ESI) available: CID mass spectrum of $[Ag_{10}D_8L_6]^{3+\bullet}$; two curve linear fit for the onset of ionization of $[Ag_{10}D_8L_6]^{2+}$; RI-PBE/RECP-def2-SVP optimised structure of isomers **II** and **III** of $[Ag_{10}H_8L_6]^{2+}$; RI-PBE/RECP-def2-SVP calculated HOMO of the isomer **I** of $[Ag_{10}H_8L_6]^{2+}$; RI-PBE/RECP-def2-SVP calculated Mulliken charges isomer **I** of $[Ag_{10}H_8L_6]^{2+}$ and $[Ag_{10}H_8L_6]^{3+\bullet}$; Cartesian coordinates of isomers **I**, **II** and **III** of $[Ag_{10}H_8L_6]^{2+}$ and of isomer **I** for $[Ag_{10}H_8L_6]^{3+\bullet}$. See DOI: 10.1039/c5cp01160d

The $[Ag_{10}H_8L_6]^{2+}$ cluster exhibits interesting unimolecular chemistry under conditions of multistage (MS^n) low energy collision-induced dissociation (CID). Initially only sequential losses of a single dppm ligand are observed in the MS^2 CID spectrum (eqn (1)) and the in the MS^3 CID spectrum (eqn (2)).[3b] Isolation of $[Ag_{10}H_8L_4]^{2+}$ followed by another stage of CID leads to a series of even-electron, singly charged ligated silver hydride fragment ions in the in the MS^4 spectrum. These arise from fission of the cluster core, with some being complementary fragment ions arising from direct core fission (*e.g.* $[AgL_2]^+$ and $[Ag_9H_8L_2]^+$, eqn (3)) while others arise from the initial loss of a ligand (*e.g.* $[Ag_3H_2L]^+$ and $[Ag_7H_6L_2]^+$, eqn (4)). To better understand how the structure of this cluster is related to its chemistry, here we present the first use of VUV ion yield spectroscopy[6] to probe the photoionisation and photofragmentation of $[Ag_{10}D_8L_6]^{2+}$ in the gas phase, while Density Functional Theory (DFT) was used to characterise its structure.

$$[Ag_{10}H_8L_6]^{2+} \rightarrow [Ag_{10}H_8L_5]^{2+} + L \quad (1)$$

$$[Ag_{10}H_8L_5]^{2+} \rightarrow [Ag_{10}H_8L_4]^{2+} + L \quad (2)$$

$$[Ag_{10}H_8L_4]^{2+} \rightarrow [AgL_2]^+ + [Ag_9H_8L_2]^+ \quad (3)$$

$$\rightarrow [Ag_3H_2L]^+ + [Ag_7H_6L_2]^+ + L \quad (4)$$

Results and discussion

Products formed upon irradiation of $[Ag_{10}D_8L_6]^{2+}$ by VUV radiation

ESI-MS of a 50 μM methanol : chloroform (1 : 1) solution of $AgBF_4$ and dppm at a molar ratio of 1 : 1 and 30 minutes after the addition of 5 molar equivalents of sodium borodeuteride produced the desired cluster, $[Ag_{10}D_8L_6]^{2+}$, together with other silver containing cluster cations as previously reported.[3b,5a] Sodium borodeuteride was used as a source of isotopically labelled hydride as it allows fragmentation losses attributed to hydride to be distinguished from those involving the dppm ligand.[3b] Mass selection of only $[Ag_{10}D_8L_6]^{2+}$ (*m*/*z* 1701) in an ion trap followed by irradiation with 15.5 eV VUV radiation resulted in the mass spectrum shown in Fig. 1. Key product ions observed include: $[Ag_{10}D_8L_5]^{2+}$, $[Ag_{10}D_8L_4]^{2+}$, $[Ag_{10}D_8L_6]^{3+\bullet}$, $[Ag_9D_8L_4]^{2+\bullet}$, and $[AgL_2]^+$. The first two ions arise from photodissociation and are related to the sequential ligand losses observed under conditions of CID (*cf.* eqn (1) and (2)).[3b] The remaining three ions appear to be related by photoionisation (eqn (5) and (6)). The unusual peak shapes observed for $[Ag_{10}D_8L_6]^{3+\bullet}$ and $[Ag_9D_8L_4]^{2+\bullet}$ are caused by ion fragmentation upon ejection from the ion trap and detection, and are thus consistent with these ions being "fragile" and undergoing metastable fragmentation.[7] Indeed, CID of $[Ag_{10}D_8L_6]^{3+\bullet}$ (Fig. S1, ESI†) confirms that $[Ag_9D_8L_4]^{2+\bullet}$ and $[AgL_2]^+$ arise from fragmentation of $[Ag_{10}D_8L_6]^{3+\bullet}$ (eqn (6)). This type of asymmetric fragmentation has been observed for the silver hydride dication, $[Ag_{10}H_8L_4]^{2+}$,[3b,8] and well as for multiply charged bare metal silver and gold cluster cations.[9]

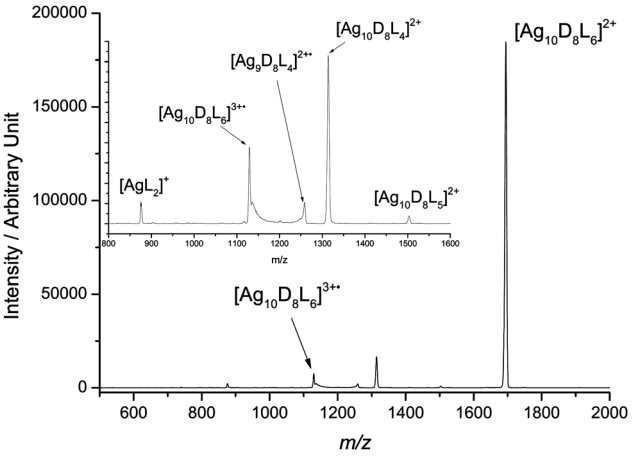

Fig. 1 LTQ ESI-MS/MS of the mass selected silver cluster dication, $[Ag_{10}D_8L_6]^{2+}$ irradiated at 15.5 eV for a period of 200 ms. The inset shows an expansion of the photoionisation and photofragmentation products.

$$[Ag_{10}D_8L_6]^{2+} + h\nu \rightarrow [Ag_{10}D_8L_6]^{3+\bullet} + e^- \quad (5)$$

$$[Ag_{10}D_8L_6]^{3+\bullet} \rightarrow [AgL_2]^+ + [Ag_9D_8L_4]^{2+\bullet} \quad (6)$$

Product ion yields as a function of the irradiation energy

We next examined the yields of these product ions as a function of the photon energy used (Fig. 2). The following conclusions can be drawn from this data: (i) the relative yields of all product ions are photon energy-dependent; (ii) $[Ag_{10}D_8L_5]^{2+}$ is formed at low energies *via* ligand loss (Fig. 2a); (iii) the onset for the formation of $[AgL_2]^+$ and $[Ag_9D_8L_4]^{2+\bullet}$ is between 1–2 eV higher than that for ionisation to produce $[Ag_{10}D_8L_6]^{3+\bullet}$ (Fig. 2b). If fragmentation *via* eqn (6) is exothermic, then the difference in onset would be due to the presence of a reverse Coulomb barrier.[10] In contrast, if fragmentation *via* eqn (6) is endothermic, then the difference in onset would be due to a threshold for fragmentation. Note that the very similar curves for the $[Ag_9D_8L_4]^{2+\bullet}$ and $[AgL_2]^+$ yields suggest that whatever the nature of the reaction, these two ions originate from the same precursor and are formed together *via* a unimolecular process, which is also consistent with the CID spectrum of $[Ag_{10}D_8L_6]^{3+\bullet}$ (Fig. S1, ESI†).

Determination of the onset for ionisation of $[Ag_{10}D_8L_6]^{2+}$

Since the ionisation energy of coinage metal nanoclusters has been related to their structures,[11] the onset for ionisation of $[Ag_{10}D_8L_6]^{2+}$ was determined from a linear fit of the yield of the product ion, $[Ag_{10}D_8L_6]^{3+\bullet}$, as a function of the VUV energy used. The photoionisation curve displays two slopes (Fig. S2, ESI†). The onset of ionisation obtained from the intercept of the linear fit of the lower energy slope is 9.3 ± 0.3 eV, while that of the second slope is 10.6 ± 0.4 eV.

The presence of two slopes associated with ionisation may be explained by the removal of electrons from different orbitals, the first slope arising from removal of an electron from the HOMO orbital and the second one from removal of electron(s) localised deeper in the valence shell, as has been noted for

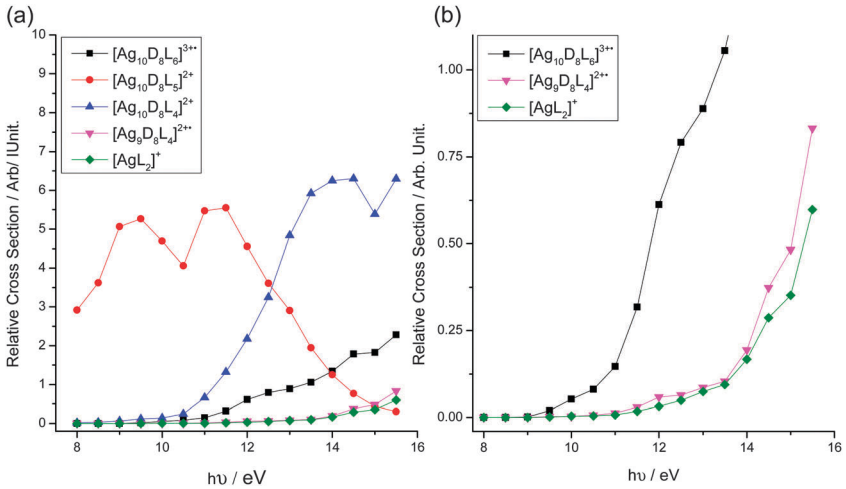

Fig. 2 (a) LTQ ESI-MS/MS yields of the product ions, $[Ag_{10}D_8L_5]^{2+}$, $[Ag_{10}D_8L_4]^{2+}$, $[Ag_{10}D_8L_6]^{3+\bullet}$, $[Ag_9D_8L_4]^{2+\bullet}$, and $[AgL_2]^+$ formed from irradiation of $[Ag_{10}D_8L_6]^{2+}$ for a period of 200 ms as a function of the VUV irradiation energy, which was varied from 8 to 15.5 eV, (b) expansion of the *y* axis to show the difference in the onset of ionisation *versus* formation of $[AgL_2]^+$ and $[Ag_9D_8L_4]^{2+\bullet}$.

ionisation of lithium clusters.[13] One cannot exclude other contributions such as thermal effects or the possibility of the presence of more than one structural isomer of the cluster.

DFT calculations relating the ionisation energy of $[Ag_{10}D_8L_6]^{2+}$ to its structure

The experimentally determined onset of ionisation of $[Ag_{10}D_8L_6]^{2+}$ provides an opportunity to test potential structures of $[Ag_{10}D_8L_6]^{2+}$ determined *via* DFT calculation using the hydride ligated, $[Ag_{10}H_8L_6]^{2+}$ cluster. The large number of atoms (172 heavy atoms, 140 hydrogen atoms) in the $[Ag_{10}H_8L_6]^{2+}$ cluster, coupled with the challenge of sampling the wide range of isomeric structures associated with different geometries of the silver core, placement of the hydride and bisphosphine ligands, and the conformational space associated with the bisphosphine ligands represent a formidable challenge for theory. Therefore we turned to inspiration from known geometries of related clusters containing 10 or more heavy atoms in the cluster core. Based on the related *closo*-borane dianion, $[B_{10}H_{10}]^{2-}$ (ref. 15) and zintyl cluster ions,[16] which are known to have compact structures related to idealised platonic solids in which the heavy atoms are located at vertices, we have used two Johnson solids,[17] the elongated square bipyramid (Johnson solid J_{15}) and the bicapped square antiprism (J_{17}), which contain 10 vertices as a starting guess for the location of the silver atoms. The hydrides were then placed at faces of these structures, thus each binding to three silver atoms as a μ_3 ligand. The 6 bisphosphine ligands were then placed such that 4 of the ligands were bound as bidentate ligands bridging two different silver atoms, while the remaining two were bound through only 1 phosphine site to the apical silver atoms (Fig. 3b). The resulting structures were then fully optimised without any symmetry constraints employing DFT method at the RI-PBE/RECP-def2-SVP level of theory[19–22] using the Turbomole[18] program. The level of the theory is a compromise between accuracy and the computational time required for full geometry optimizations. The structure with J_{17} core has the lowest energy while the system with the J_{15} core transforms during geometry optimization into the lowest energy structure with J_{17} core.

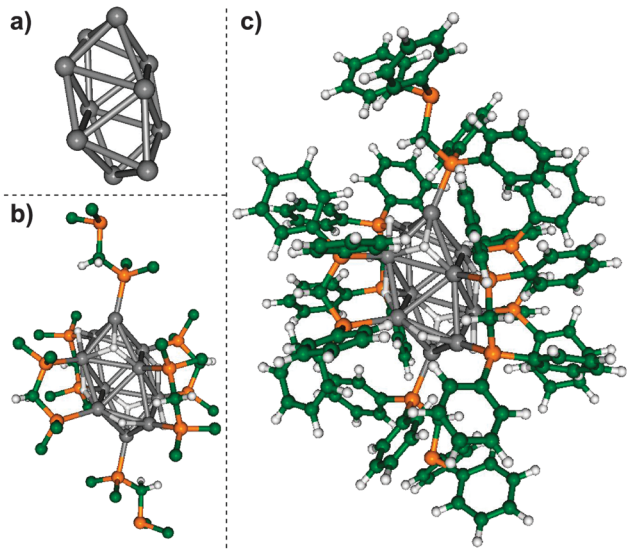

Fig. 3 RI-PBE/RECP-def2-SVP optimised structure of the isomer **I** of $[Ag_{10}H_8L_6]^{2+}$. (a) Bicapped square antiprism (J_{17}) silver cluster core. (b) Part of the fully optimised system showing the core, hydrides and "first shell" of dppm ligands. The phenyl ring and H atoms of dppm ligand have been omitted. (c) Structure of fully optimised system. Grey, orange, white and green colours label silver, phosphorus, hydrogen and carbon atoms.

The lowest energy structure, isomer **I** (Fig. 3), contains a symmetric bicapped square antiprism structure as a core (Fig. 3a). In the structure containing the core, hydrides and "first shell" of dppm shown in Fig. 3b the core remains unchanged. The hydrides have two different coordination modes; 4 μ_2 hydride ligands: and 4 μ_3 hydride ligands. Isomer **II**, which is 0.27 eV higher in energy, contains a non-symmetric distorted bicapped

square antiprism as its core (Fig. S3a, ESI†). For isomer **III**, which is 0.91 eV higher in energy than isomer **I**, the silver core consists of two distorted trigonal bipyramids, with an apical silver atom of one bipyramid bridging an apical and an equatorial silver atom of the other bipyramid (Fig. S3b, ESI†).

Although there is no guarantee that we have found the most stable structure of the cluster, the calculated vertical ionisation energy for isomer **I** is 8.7 eV. The HOMO of the cluster is delocalised over the cluster core (Fig. S4, ESI†). According to the Mulliken analysis, the positive charge is localised at the silver-phosphorus atoms located at the top of bicapped square antiprism (Fig. S5, ESI†). The geometry optimization of $[Ag_{10}H_8L_6]^{3+\bullet}$ led to the structure presented in Fig. S5 (ESI†) in which the silver core together with the neighbouring atoms are closely related to the structure for the dication. Moreover, the HOMO of the trication is also delocalised over the cluster core, while the third positive charge is delocalised on phenyl rings. Consequently, the calculated adiabatic ionisation energy IE_a is 8.54 eV, which is only ~0.2 eV lower than vertical ionisation energy, in satisfactory agreement with experimentally determined ionisation energy. These ionisation energies are significantly lower than the 2nd and 3rd ionisation energies of bare silver cluster cations,[12] which are in the 19–20.2 eV range for Ag_x^{2+} (x = 17, 21, 29 and 43).[12a] This highlights the role of the hydride and dppm ligands in lowering the ionisation energy.

Experimental

Materials

Chemicals from the following suppliers were used without further purification: (i) Aldrich: bis(diphenylphosphino)-methane (dppm, L) (97%), silver(I) tetrafluoroborate ($AgBF_4$) (98%), sodium borodeuteride ($NaBD_4$) (98% D, 90% CP); (ii) Sigma: methanol (AR grade for synthesis and HPLC grade for ESI-MS^n experiments), acetonitrile (HPLC grade).

Synthesis of $[Ag_{10}D_8L_6]^{2+}$

The $[Ag_{10}D_8L_6]^{2+}$ was prepared as previously reported.[3b,5a]

Mass spectrometry

Mass spectrometry experiments were conducted on a Finnigan LTQ linear ion trap mass spectrometer that has been coupled to the DESIRS beamline of the SOLEIL synchrotron.[14] This undulator beamline produced a high flux of photon (typically in the 10^{12}–10^{13} ph per s per 0.1% bandwidth), tunable over the whole VUV range (5–40 eV) with a high spectral purity, *i.e.* with no high harmonics of the undulator that could be transmitted by the gratings' high orders, and which are very efficiently cut-off by a gas filter. This is a crucial issue in the context of the mass spectrometry experiments. All photon-energy spectra have been normalised to the incident photon flux owing to a dedicated photodiode (IRD AXUV100). The condensed phase silver cluster samples were typically diluted in methanol to silver concentrations of 50 μM and injected at a flow rate 5 μL min^{-1} into the Finnigan ESI source. ESI source conditions typically involved needle potentials of 3.2–4.8 kV to give a stable source current of *ca.* 0.5 μA and a nitrogen sheath gas pressure of 5 arbitrary units. The ion transfer capillary temperature was set to 250 °C. The tube lens voltage and capillary voltage were both set to *ca.* 10.0 V. Unimolecular fragmentation studies involved the cation of interest being mass selected in the linear ion trap (LIT) by a range of 10–20 m/z units centered at *ca.* the middle of the isotopic cluster and subsequently analyzed by CID.

DFT calculations

The Turbomole[18] program was used with the PBE RI functional[19,20] and the RECP basis set for silver atoms[21] and the SVP basis set for all other atoms[22] to fully optimise the cluster and to determine its vertical and adiabatic ionisation energy. The latter was determined by fully optimising the $[Ag_{10}H_8L_6]^{3+\bullet}$ cluster using the optimised structure of $[Ag_{10}H_8L_6]^{2+}$ cluster as the starting geometry.

Conclusions

This is the first report to have used VUV radiation to examine the ionisation and fragmentation of the ligated silver deuteride nanocluster cation, $[Ag_{10}D_8L_6]^{2+}$. The ionisation of $[Ag_{10}D_8L_6]^{2+}$, monitored by the yield of the product ion, $[Ag_{10}D_8L_6]^{3+\bullet}$ as a function of the VUV energy, required a two curve linear fit. The experimentally determined ionisation energy of $[Ag_{10}D_8L_6]^{2+}$ is 9.3 ± 0.3 eV. This 3rd ionisation energy is considerably lower than the 2nd and 3rd ionisation energies of bare silver cluster cations, highlighting the key role of the ligands in stabilising the charge. It will be interesting to systematically examine the role of cluster stoichiometry on the ionisation energy of other ligated silver hydride cluster cations.

The DFT calculated adiabatic ionisation of $[Ag_{10}H_8L_6]^{2+}$ was determined to be 8.54 eV, in satisfactory agreement with the experimentally determined value. Moreover, the DFT calculated structure of $[Ag_{10}H_8L_6]^{2+}$ is consistent with the following experimental observations:

(1) the $[Ag_{10}H_8L_6]^{2+}$ fragments *via* sequential loss of two dppm ligands under CID conditions in the gas phase (eqn (1)). The two ligands lost are likely to be those that only bind *via* one phosphine group to a single Ag atom of the cluster.

(2) $[Ag_{10}H_8L_6]^{2+}$ is only stable for less than a day in the condensed phase, which may be due to the potential for these free phosphorus donor sites to bind to silver(I) ions or nanoclusters of various nuclearity due to dynamic processes such as Ostwald ripening and agglomeration.

Finally, the coupling of a commercial linear ion trap mass spectrometer with electrospray ionization with VUV radiation from a synchrotron source provides an unique instrument to examine the photoionisation and photofragmentation reactions of metal nanoclusters. It adds to the arsenal of techniques available to examine the fundamental properties and reactions of metal nanoclusters.

Acknowledgements

We thank the Australian Research Council for financial support (DP150101388, and *via* the ARC CoE for Free Radical Chemistry and Biotechnology), Prof. Paul Mulvaney for his ongoing support and interest in this nanocluster work and Assoc. Prof. Brendan Abrahams for useful discussions on possible structures of the $[Ag_{10}H_8L_6]^{2+}$ cluster. R.A.J.O. thanks The Université de Lyon for a visiting Professorship and the School of Chemistry at the University of Melbourne for a short-term study leave. SOLEIL support is acknowledged under project no. 20121299. We also thank the general technical staff of SOLEIL for running the facility. AZ acknowledges the award of an Australian Postgraduate PhD Scholarship. The research leading to these results has received funding from the European Research Council under the European Union's Seventh Framework Programme (FP7/2007–2013 Grant agreement No. 320659). VBK and MK acknowledge Prof. Miroslav Radman at MedILS and Split-Dalmatia County for kind support.

References

1 (*a*) G. N. Khairallah and R. A. J. O'Hair, *Angew. Chem., Int. Ed.*, 2005, **44**, 728; (*b*) G. N. Khairallah and R. A. J. O'Hair, *Dalton Trans.*, 2005, 2702; (*c*) G. N. Khairallah and R. A. J. O'Hair, *Dalton Trans.*, 2007, 3149; (*d*) G. N. Khairallah and R. A. J. O'Hair, *Dalton Trans.*, 2008, 2956; (*e*) F. Q. Wang, G. N. Khairallah and R. A. J. O'Hair, *Int. J. Mass Spectrom.*, 2009, **283**, 17; (*f*) W. A Donald and R. A. J. O'Hair, *Dalton Trans.*, 2012, **41**, 3185.

2 (*a*) T. Baba, N. Komatsu, H. Sawada, Y. Yamaguchi, T. Takahashi, H. Sugisawa and Y. Ono, *Langmuir*, 1999, **15**, 7894; (*b*) K. Shimizu, R. Sato and A. Satsuma, *Angew. Chem., Int. Ed.*, 2009, **48**, 3982; (*c*) K. Shimizu, K. Sugino, K. Sawabe and A. Satsuma, *Chem. – Eur. J.*, 2009, **15**, 2341; (*d*) K. Shimizu and A. Satsuma, *J. Jpn. Pet. Inst.*, 2011, **54**, 347; (*e*) A. A. Gabrienko, S. S. Arzumanov, I. B. Moroz, A. V. Toktarev, W. Wang and A. G. Stepanov, *J. Phys. Chem. C*, 2013, **117**, 7690.

3 (*a*) R. Mitrić, J. Petersen, A. Kulesza, M. Röhr, V. Bonačić-Koutecký, C. Brunet, R. Antoine, P. Dugourd, M. Broyer and R. A. J. O'Hair, *J. Phys. Chem. Lett.*, 2011, **2**, 548; (*b*) M. Girod, M. Krstić, R. Antoine, L. MacAleese, J. Lemoine, A. Zavras, G. N. Khairallah, V. Bonačić-Koutecký, P. Dugourd and R. A. J. O'Hair, *Chem. – Eur. J.*, 2014, **20**, 16626.

4 (*a*) C. W. Liu, H. W. Chang, C. S. Fang, B. Sarkar and J. C. Wang, *Chem. Commun.*, 2010, **46**, 4571; (*b*) C. W. Liu, H.-W. Chang, B. Sarkar, J.-Y. Saillard, S. Kahlal and Y.-Y. Wu, *Inorg. Chem.*, 2010, **49**, 468; (*c*) C. W. Liu, P.-K. Liao, C.-S. Fang, J.-Y. Saillard, S. Kahlal and J.-C. Wang, *Chem. Commun.*, 2011, **47**, 5831; (*d*) J. H. Liao, C. Latouche, B. Li, S. Kahlal, J.-Y. Saillard and C. W. Liu, *Inorg. Chem.*, 2014, **53**, 2260; (*e*) B. K. Tate, C. M. Wyss, J. Bacsa, K. Kluge, L. Gelbaum and J. P. Sadighi, *Chem. Sci.*, 2013, **4**, 3068; (*f*) C. Latouche, S. Kahlal, Y. R. Lin, J. H. Liao, E. Furet, C. W. Liu and J.-Y. Saillard, *Inorg. Chem.*, 2013, **52**, 13253.

5 (*a*) A. Zavras, G. N. Khairallah, T. U. Connell, J. M. White, A. J. Edwards, P. S. Donnelly and R. A. J. O'Hair, *Angew. Chem., Int. Ed.*, 2013, **52**, 8391; (*b*) A. Zavras, G. N; Khairallah, T. U. Connell, J. M. White, A. J. Edwards, R. J. Mulder, P. S. Donnelly and R. A. J. O'Hair, *Inorg. Chem.*, 2014, **53**, 7429; (*c*) A. J. Clark, A. Zavras, G. N. Khairallah and R. A. J. O'Hair, Bis(dimethylphosphino)methane-Ligated Silver Chloride, Cyanide and Hydride Cluster Cations: Synthesis and Gas-Phase Unimolecular Reactivity, *Int. J. Mass Spectrom.*, 2015, DOI: 10.1016/j.ijms.2014.07.015.

6 For VUV ionisation studies of multiply charged biomolecular ions using the SOLEIL synchrotron see: (*a*) A. R. Milosavljević, C. Nicolas, J. Lemaire, C. Dehon, R. Thissen, J.-M. Bizau, M. Réfrégiers, L. Nahon and A. Giuliani, *Phys. Chem. Chem. Phys.*, 2011, **13**, 15432; (*b*) A. Giuliani, A. R. Milosavljević, K. Hinsen, F. Canon, C. Nicolas, M. Réfrégiers and L. Nahon, *Angew. Chem., Int. Ed.*, 2012, **51**, 9552; (*c*) O. González-Magaña, G. Reitsma, M. Tiemens, L. Boschman, R. Hoekstra and T. Schlathölter, *J. Phys. Chem. A*, 2012, **116**, 10745; (*d*) C. Brunet, R. Antoine, P. Dugourd, F. Canon, A. Giuliani and L. Nahon, *J. Chem. Phys.*, 2013, **138**, 064301.

7 The act of ejecting ions from an ion trap during the mass analysis stage can impart a small amount of energy to the ions. If these ions are fragile, they become metastable, which gives rise to a characteristic peak shape due to differences in arrival times to the detector. For a description of peak fronting, see: J. P. Murphy and R. A. Yost, *Rapid Commun. Mass Spectrom.*, 2000, **14**, 270.

8 A. Kulesza, R. Mitric, V. Bonacic-Koutecky, B. Bellina, I. Compagnon, M. Broyer, R. Antoine and P. Dugourd, *Angew. Chem., Int. Ed.*, 2011, **50**, 878.

9 (*a*) S. Krückeberg, G. Dietrich, K. Lützenkirchen, L. Schweikhard, C. Walther and J. Ziegler, *Hyperfine Interact.*, 1997, **108**, 107; (*b*) J. Ziegler, G. Dietrich, S. Krückeberg, K. Lützenkirchen, L. Schweikhard and C. Walther, *Hyperfine Interact.*, 1999, **115**, 171; (*c*) S. Krückeberg, G. Dietrich, K. Lützenkirchen, L. Schweikhard, C. Walther and J. Ziegler, *Z. Phys. D*, 1997, **40**, 341; (*d*) S. Krückeberg, L. Schweikhard, G. Dietrich, K. Lützenkirchen, C. Walther and J. Ziegler, *Chem. Phys.*, 2000, **262**, 105.

10 (*a*) F. Garcias, J. A. Alonso, J. M. López and M. Barranco, *Phys. Rev. B: Condens. Matter Mater. Phys.*, 1991, **43**, 9459; (*b*) F. Chandezon, C. Guet, B. A. Huber, D. Jalabert, M. Maurel, E. Monnand, C. Ristori and J. C. Rocco, *Phys. Rev. Lett.*, 1995, **74**, 3784; (*c*) U. Näher, S. Bjørnholm, S. Frauendorf, F. Garcias and C. Guet, *Phys. Rep.*, 1997, **285**, 245.

11 W. A. De Heer, *Rev. Mod. Phys.*, 1993, **65**, 611.

12 (*a*) I. Rabin and W. Schulze, *Chem. Phys. Lett.*, 1993, **201**, 265; (*b*) A. Halder, A. Liang, C. Yin and V. V. Kresin, *J. Phys.: Condens. Matter*, 2012, **24**, 104009.

13 P. Dugourd, D. Rayane, P. Labastie, B. Vezin, J. Chevaleyre and M. Broyer, *Chem. Phys. Lett.*, 1992, **197**, 433.

14 (*a*) L. Nahon, N. de Oliveira, G. A. Garcia, J.-F. Gil, B. Pilette, O. Marcouillé, B. Lagarde and F. Polack, *J. Synchrotron Radiat.*,

2012, **19**, 508; (*b*) A. R. Milosavljević, C. Nicolas, J. Gil, F. Canon, M. Réfrégiers, L. Nahon and A. Giuliani, *J. Synchrotron Radiat.*, 2012, **19**, 174.
15 I. B. Sivaev, A. V. Prikaznov and D. Naoufal, *Collect. Czech. Chem. Commun.*, 2010, **75**, 1149.
16 S. Scharfe, F. Kraus, S. Stegmaier, A. Schier and T. F. Fässler, *Angew. Chem., Int. Ed.*, 2011, **50**, 3630.
17 N. W. Johnson, *Canad. J. Math.*, 1966, **18**, 169.
18 TURBOMOLE V6.4 2012, a development of University of Karlsruhe and Forschungszentrum Karlsruhe GmbH, 1989–2007, TURBOMOLE GmbH, since 2007, available from www.turbomole.com.
19 J. P. Perdew, K. Burke and M. Ernzerhof, *Phys. Rev. Lett.*, 1996, **77**, 3865.
20 K. Eichkorn, O. Treutler, H. Öhm, M. Häser and R. Ahlrichs, *Chem. Phys. Lett.*, 1995, **242**, 652.
21 D. Andrae, U. Haeussermann, M. Dolg, H. Stoll and H. Preuss, *Theor. Chim. Acta*, 1990, **77**, 123.
22 F. Weigend and R. Ahlrichs, *Phys. Chem. Chem. Phys.*, 2005, **7**, 3297.